Study of the response of CFRP composite laminates to a laser-induced shock

Elise Gay [a,*], Laurent Berthe [a], Michel Boustie [b], Michel Arrigoni [c], Marion Trombini [b]

[a] Laboratoire Procédés et Ingénierie en Mécanique et Matériaux (CNRS), Arts et Métiers ParisTech, 151 bd de l'Hôpital, 75013 Paris, France
[b] Département Physique et Mécanique des Matériaux, Institut Pprime (CNRS) ENSMA, 1 av. Clément Ader, 86960 Futuroscope Cedex, France
[c] Laboratoire Brestois de Mécanique et des Systèmes EA 4325, ENSTA-Bretagne, 2 rue François Verny, 29806 Brest Cedex 9, France

A B S T R A C T

Laser-induced shock yields to a local tensile stress within a sample. This high strain rate stress can be used to verify the bond strength between two layers. This method has been applied to Carbon Fibre Reinforced Polymer (CFRP) composite laminates, involved in aeronautic or defense industry. Experiments have been carried out on high power laser facility in the nanosecond regime. A velocimetry interferometer has been used to record the material velocity at the back surface of the samples. This study provides a comprehensive approach of the response of CFRP laminates of different thicknesses to a shock load normal to the fibres direction. The stress waves generation and propagation within the laminate and the induced delamination are key issues of this work. The main result is the ability of the technique to evaluate the out-of-plane strength of these laminates.

Keywords:
A. Laminates
B. Adhesion
B. Impact behaviour
D. Non-destructive testing
Shock wave

1. Introduction

In a context of rising use of composite materials, the assessment of their strength is a key issue for the aircraft industry. Strength deterioration is induced by improper surface preparation or contamination, by the accidental inclusion of a separator film in the lay-up. Composites left out of storage too long before the curing also reduce adhesion between plies. Local strength degradation cannot be detected using conventional Non-Destructive Inspection methods since there is no noticeable separation between plies [1]. The measurement of the strength requires the destruction of the part.

A proof-test using laser-induced shock in the ns regime is proposed to verify the bond strength between plies. It has the ability to generate a calibrated tensile stress within a target with a stain rate of about $10^6\ s^{-1}$. Numerical simulation of the experiments provides an evaluation of the stress.

Since the first demonstration by Vossen [2], the adhesion test using laser-induced shock has been performed many times to evaluate the adhesion strength. It concerns thin coatings [3–5], and bonded assemblies [6,7]. The potential disbond is detected using the non-intrusive measurement of the free surface velocity [8,9] or ultrasonic C-scan [10].

Relatively few studies describe the application of this process to CFRP composites: Gupta has investigated the adhesion test between plies [11] and between the fibres and their matrix [12]. Gilath has also studied the response of unidirectional CFRP composites to a laser-induced shock [13,14]. The SATAC research program (Shock Adhesion Test for Adhesively Bonded Composites) aims to study the composites behaviour at very high strain rate in order to test their adhesion [15–17]. Other studies describe the behaviour of CFRP laminates under plate impact in the through-thickness direction [18], and along the fibre direction [19,20]. The response of glass fibers reinforced epoxy [21,22] Kevlar/epoxy and Spectra/epoxy composites [23] to a planar impact has also been investigated.

In this context, this work reports the development effort to characterize the response of aerospace-grade CFRP laminates to a laser-induced shock normal to the fibre direction (out-of-plane). Two thickness configurations are studied to demonstrate the feasibility of the adhesion test and evaluate the dynamic through-thickness strength of a laminate. The study investigates three major points: the generation of laser-induced shock on CFRP composites, the propagation of high-intensity stress waves within these multi-layer materials, and the resulting delamination.

This article is divided into seven sections. Section 2 describes the CFRP laminates involved in this study. The next section introduces the adhesion test between plies based on laser-induced shock. The response of 4 and 8 ply laminates has been investigated

* Corresponding author.
E-mail address: elise.gay@hotmail.fr (E. Gay).

at very high strain rate, respectively in Sections 4 and 5. A discussion of the advantages and drawbacks of the application of the process to composite laminates concludes this article.

2. CFRP laminates

CFRP composites are extensively used in modern aircraft structures due to their high strength-to-weight ratio. The materials chosen for this study are CFRP laminates that have been manufactured using the carbon fibres G40-800-24 K reinforced epoxy Cytec® 5276-1. Baseline materials are 4 and 8 ply laminates with a lay-up sequence of respectively $[0°/90°]_S$ and $[0/-45/90/45°]_S$, and an approximate thickness of 600 and 1200 µm. They are cut to 15 × 15 mm samples. These materials are representative of industrial applications in aeronautic field.

Fig. 1 shows their cross-sections in the through-thickness direction, the fibres of the external plies are orthogonal to the cutting plane. The average diameter of the carbon fibres is 5 µm, their volume fraction is 70%. A 30 µm thick interply provides adhesion between plies. This epoxy layer is also observed at the surface of the laminate.

The dynamic behaviour of the composites is described using a linear-elastic law [24,22]. Properties are given in Table 1. The homogenized wave sound velocity C_0 in the transverse direction of the laminate is calculated at 2890 m s^{-1} on average. The acoustic impedance Z is defined as the product of the material density and its sound velocity.

3. Adhesion test using laser-induced shock

3.1. Principle of the test

The load is generated by a Nd:YAG laser from Continuum (PIMM laboratory, Arts et Métiers ParisTech). It delivers a calibrated pulse with a τ_{laser} = 9.3 ns duration at Full Width at Half Maximum (FWHM) and an energy of E = 1.5 J at λ = 532 nm. The laser beam is focused on a horizontal target using a position-adjustable lens. The incident energy is adjusted by a $\lambda/4$ plate and a polarizer with a 2% precision. The incident intensity is given by $I = E/\tau_{laser} \cdot S$ (S is the area of the laser spot).

The irradiated surface is rapidly vaporized into a high pressure plasma, inducing a compressive stress wave within the sample. The plasma is confined using a thin water overlay, that increases the pressure (from 5 to 10 times) and the pulse duration (from 2 to 3 times) [25,26]. A transparent adhesive tape could replace the water overlay to confine the plasma. The incident surface of the laminate is protected from the irradiation by a sacrificial thin layer of black paint [27].

The high intensity pulse drives a compression wave within the specimen to test, followed at the end of the load by a release wave that relaxes the material to its initial state. This pulse propagates within the sample thickness to the opposite surface, where it is reflected back in tension (see Fig. 5a). This stress is able to induce damage (see Fig. 5b), depending on its amplitude and duration [9].

The proof-test uses this high strain rate tensile stress to load locally the interface between two layers. A strong interface will remain unaffected under a calibrated load whereas a weak one will fail, creating an internal disbond detectable using a velocimetry interferometer at the surface opposite to the impact. Each compressive wave reaching the free surface accelerates it, and conversely the arrival of a tensile wave induces a deceleration. The velocity at the free surface of the sample provides thus useful information about the propagation of the waves. It indicates whether a wave has been isolated and reflected within a delaminated portion of the sample. A VISAR (Velocimetry Interferometer System for Any Reflector [8]) is used to record the motion of the back surface. This interferometer is based on the Doppler shift of the light reflected from the free surface. Its time precision is in the ns range with a 1% error between 10 and 10^4 m s^{-1} in our configuration. A typical experimental set-up is given schematically in Fig. 2.

In the context of this study, the microscopic observations and the microtomographies of the recovered targets confirm the absence or presence of shock-induced damage.

This test remains non-destructive while the generated stress does not exceed a prescribed threshold. This threshold is estimated by subjecting similar samples to a shock load. The incident intensity is gradually increased until a disbond is detected. The dynamic tensile strength is then evaluated based on numerical simulations of the experiments.

Once this is achieved for reference laminates, proof tests can be performed by subjecting a designated target to a shock at a fixed intensity (below the threshold) to verify it meets minimal strength.

3.2. Load parameters

Fig. 3 reports the magnitude of the incident pressure as a function of laser intensity (Fig. 3a) and time (Fig. 3b). It depends on the material and on the wavelength and pulse duration of the laser.

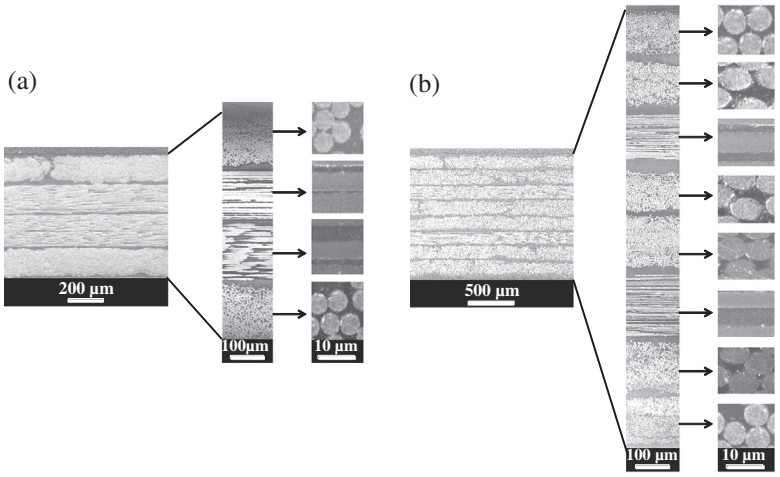

Fig. 1. Microscopic SEM observations of CFRP composites cross-section with high magnification of the plies and fibres: (a) 4 ply, and (b) 8 ply laminate.

Table 1
Material properties (*T* for transverse, *L* for longitudinal direction) [16].

	Initial density (kg m^{-3})	Young's modulus (GPa)	Poisson ratio	Sound velocity (m s^{-1})	Impedance (g cm^{-2} s^{-1})
Epoxy	1260	5.2	0.35	2600	0.33×10^6
Ply dir T	1630	12.6	0.3 (LT)	3000	0.49×10^6
dir L	1630	202	0.27 (TZ)	8100	1.32×10^6

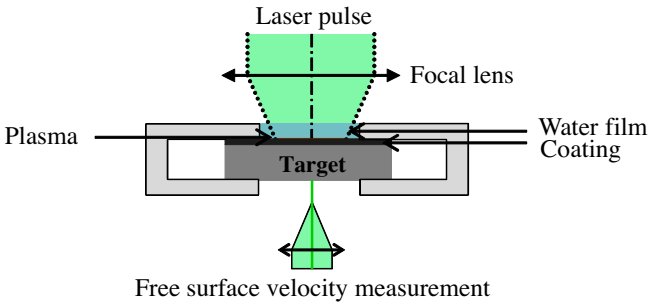

Fig. 2. Experimental set-up of the test (scale not respected).

The peak pressure P_{max} is estimated for each impact using an inverse approach: the load amplitude is adjusted as an input parameter of the model by fitting the amplitude of the experimental and numerical first velocity peak. Fig. 4 shows a comparison between these velocities at the back surface of a laminate subjected to a 0.9 GW cm^{-2} irradiation, a 360 MPa load is used here. P_{max} reaches 0.57 GPa in our conditions.

The time evolution of the incident pressure is calculated using the laser-matter interaction code ACCIC (Auto Consistent Confined Interaction Model, see [25,28] for more information). The pressure pulse duration is 16 ns at FWHM.

The conditions of the experiments are reported in Table 2. The samples are referenced A to E for the 4 ply laminates, F and G for the 8 ply. They have been subjected to a load near their delamination threshold.

The laser spot diameter is 2.5 mm. When it is at least three times larger than the sample thickness, release waves from the load edge have a limited influence on wave propagation [29]. The stress waves propagate normal to the interfaces and the induced deformation is considered uniaxial at the center of the sample (mode I).

3.3. Stress wave propagation within a laminate

Unlike isotropic materials, the wave propagation within composite laminates is complex. Between each layer of the laminate, the stress wave is both transmitted and reflected depending on the impedance mismatch at the interface [24,30]. Relation (1) gives an analytical expression of the amplitude of the transmitted P_T and reflected P_R stress wave as a function of the incident wave P_{max} while crossing an interface from material A to B.

$$P_T = \frac{2Z_B}{Z_A + Z_B} P_{max}, \quad P_R = \frac{Z_B - Z_A}{Z_A + Z_B} P_{max} \tag{1}$$

The crossing of n successive plies reduces the amplitude of the incident wave to $P(n)$, given by:

$$P(n) = P_{max} \cdot \left(\frac{4Z_{ply} \cdot Z_{interply}}{(Z_{ply} + Z_{interply})^2} \right)^n \tag{2}$$

With the values from Table 1, $P(n) = P_{max} \times 0.966^n$. The material anisotropy also affects the waves propagation and the shock-induced damage [31,20].

The waves propagation within a 4 ply laminate is represented on a space–time diagram in Fig. 5a. The stress history is computed in the through-thickness direction, compression is represented in red and tensile stress in blue. The time origin corresponds to the impact on the incident surface. The laminates are represented by oriented plies between thin isotropic epoxy layers, with properties given in Table 1. The layers thicknesses (considered constant) are measured on the laminates cross-sections. Since the experimental and numerical results have the same time evolution with minor amplitude discrepancies (see Fig. 4), this computation is considered accurate. The delamination is modeled using a cut-off criterion in Fig. 5b: it occurs when the tensile stress in the through-thickness direction is higher than a prescribed level.

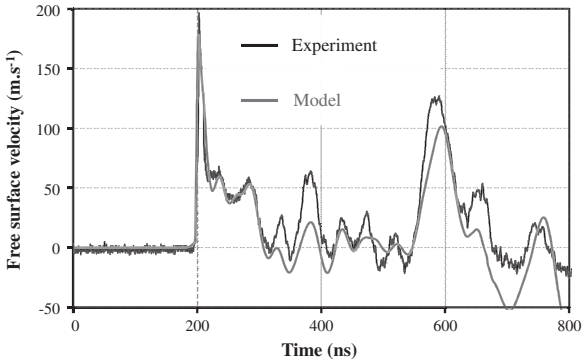

Fig. 4. Experimental and computed velocity at the rear surface of a 4 ply laminate (ABAQUS© explicit simulation, mesh size 2 µm, step time 1 ns, details of the model can be found in [16]).

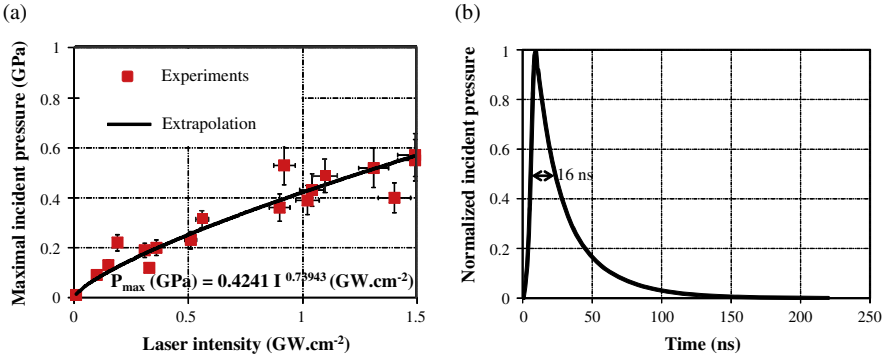

Fig. 3. Load parameters: (a) incident peak pressure as a function of laser intensity (the error bars indicate the uncertainty in the measurement of the laser energy, pulse duration and irradiated surface), and (b) time evolution of the load.

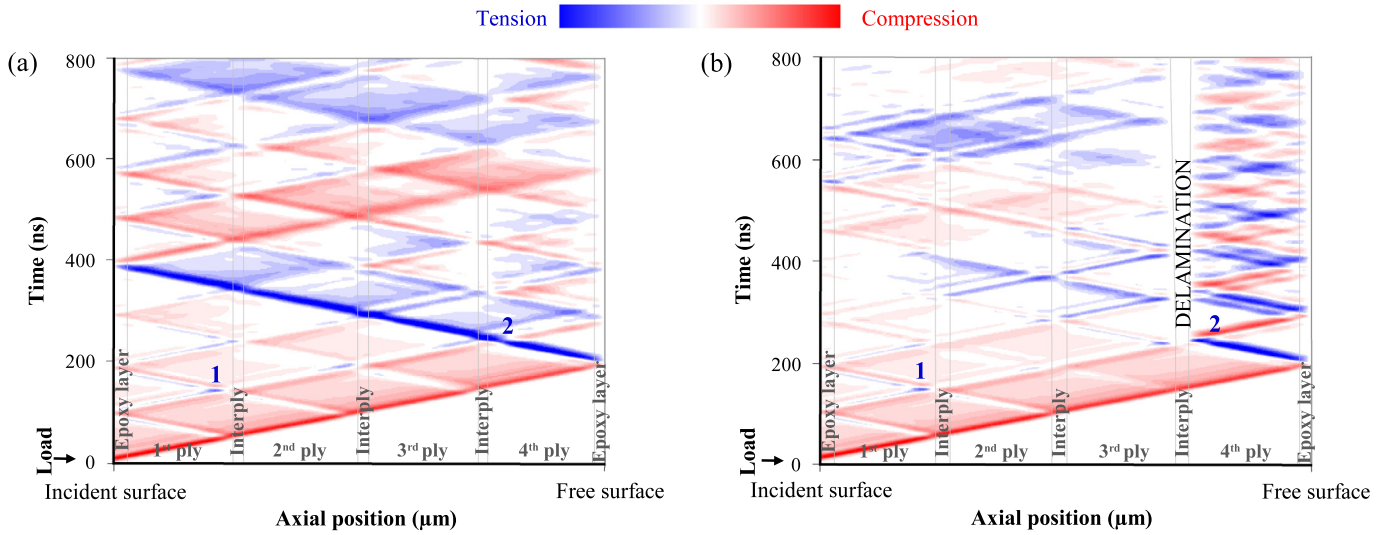

Fig. 5. Stress wave propagation within a 4 ply laminate. The stress is given on a space–time diagram as a function of time and thickness, compression in red, tensile stress in blue (ABAQUS© explicit simulation). (a) No delamination, and (b) shock-induced delamination. (For interpretation of the references to colour in this figure legend, the reader is referred to the web version of this article.)

Table 2
Parameters of the experiments performed on composites laminates.

Ref.	Shock parameters		Geometry		
	Intensity (GW cm^{-2})	Incident P_{max} (see Fig. 3a) (MPa)	Configuration	Thickness (µm)	Delamination
A	0.56	316	4 ply	690	No
B	0.90	360	4 ply	605	No
C	1.03	430	4 ply	600	Yes
D	1.10	487	4 ply	705	Yes
E	1.84	(no velocity profile)	4 ply	685	Yes
F	1.31	510	8 ply	1190	No
G	1.49	570	8 ply	1210	Yes

The stress wavelength ($\tau \times C_0 = 16 \cdot 10^{-9} \times 2890 = 4.6 \cdot 10^{-5}$ m at FWHM) is small compared with the ply thickness and the tensile stress is spread very locally.

The first important tensile stress referenced 1 at $t = 150$ ns (Fig. 5) is generated by the interaction of the reflected waves within the first and the second plies. In our configuration, it is not high enough to delaminate the composite. However, a stronger load can induce important tensile stress near the incident surface, up to delamination [16].

The tensile stress referenced 2 is generated by the reflection of the incident wave at the free surface. Its amplitude is important in the whole laminate. The interply between the 3rd and 4th ply is subjected to a high tensile stress, that is 2% lower than the stress within the 4th ply due to the relatively low impedance of the epoxy. According to the computation, this tensile stress represents 74% of the incident pressure. The tensile stress between the plies 2–3 and 1–2 is slightly lower (respectively 69% and 64% of P_{max}). The attenuation is mainly attributed to the wave reflections at the interfaces: relation (2) indicates that the reflections induce a 12.9% decrease of the stress during the first wave propagation from the incident to free surface.

In Fig. 5b, tensile stress of sufficient intensity leads to a delamination between the 3rd and 4th ply. The residual stress wave then propagates between the free surface and the delamination.

4. 4 ply laminates behaviour under laser-induced shock load

Experiments have been first performed on 4 ply laminates. Since the spot diameter is 4.2 times larger than the samples thickness, the waves propagation is considered normal to the plies and the shock front is not altered by the edge effects [32]. A delamination threshold has been probed for an incident intensity of [0.9–1.03] GW cm^{-2}. In this interval, delamination may occur for reference laminates.

The velocities recorded at the back surface of the samples B and C during the test, respectively below and above the delamination threshold, are given in Fig. 6.

The free surface velocity of sample B shows two major peaks, corresponding to the emergence of the main shock wave at the back surface. The first acceleration B_1 is induced by the incident wave front reaching the free surface, it is immediately followed by a deceleration due to rarefaction. The (assumed constant) wave

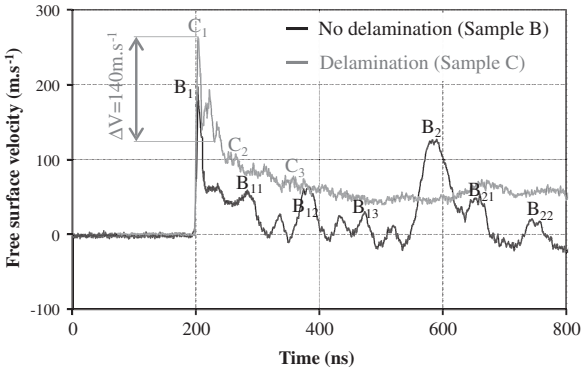

Fig. 6. Experimental free surface velocity of 4 ply laminates from 0 to 800 ns, without (sample B, 0.9 GW cm^{-2}) and with shock-induced delamination (sample C, 1.03 GW cm^{-2}). The annotations are referred to in the text.

velocity C is calculated in the transverse direction using the transit time of the shock: $C = thickness_B/t_{B1} = 605 \cdot 10^{-6}/200 \cdot 10^{-9} = 3025$ - m s^{-1}, this is approximately the homogenized sound velocity C_0 of the laminate given in Section 2. This confirms that the stress waves propagate in the elastic regime in our conditions, especially as no elastic precursor is observed on the first velocity peak B_1.

The velocity peak B_2 is generated by the main wave after propagating three times through the whole specimen (see the stress wave propagation within a 4 ply laminate in Fig. 5a). This acceleration evidences the cohesion of this sample, since it shows the wave propagates uninterruptedly through all the plies. The velocity peaks referenced B_{11} to B_{13} are generated by the wave reflections at the interfaces. Since the plies have similar thickness, the waves reflections are superimposed while reaching the back surface and their emergence is almost synchronized. Smaller unreferenced velocity peaks are induced by the numerous reflections within the interplies.

Sample C has been subjected to a stronger load above the delamination threshold. The shock-induced delamination modifies the propagation of the stress waves (see Fig. 5b) and the motion of the free surface is different from the previous case.

The first sharp rise C_1 at $t = 200$ ns is induced by the incident shock at the free surface. It is then reflected as a tensile wave that delaminates the last ply, since it is the closest to the back surface. The wave emergences C_1 to C_3 at the back surface have then a period of oscillation of 100 ns. This evidences the residual wave propagating between the free surface and the delamination at the interply 3–4.

Using the inverse approach (see Section 3.2), the delamination threshold of the 4 ply laminates is evaluated for an incident pressure of [360–430] MPa. The tensile strength at very high strain rate is then calculated at [266–318] MPa (i.e. 292 ± 26 MPa). It is given by the computed tensile stress at the interlaminar region between the 3rd and 4th ply for specimens B and C (see Section 3.3 and Fig. 5). It is much higher than the static tensile limit ([110–130] MPa [33]) due to the very high strain rate of the stress.

According to Antoun et al. [9], the dynamic tensile strength σ_{spall} is evaluated within a homogeneous material by relation (3):

$$\sigma_{spall} = \frac{1}{2}\rho_0 \times C_0 \times \Delta V \tag{3}$$

where ΔV is the experimental velocity gap (pullback) measured between the top of the first velocity peak and the take-off point. This relation is carefully applied to composites laminates. Since the small acceleration after the velocity peak C_1 is induced by a wave reflection in the outer epoxy layer (see Fig. 5b), the take-off point is defined as indicated in Fig. 6.

Here $\Delta V = 263–123 = 140$ m s^{-1} and relation (3) provides a dynamic tensile strength of $\sigma_{spall} = 342$ MPa. This value is close to the computed evaluation (292 ± 26 MPa). Thus, relation (3) provides a reliable evaluation of the laminate strength in the transverse direction, probably because the acoustic impedances of ply and interply are not so different. However, ΔV must be measured with caution.

Due to a low level of material deformation, the specimens B and C have been recovered for microscopic observation. Fig. 7a shows the cross-section micrographs of the 4 ply sample B after an impact below the delamination threshold. It does not show any damage as evidenced in the highly magnified picture near the Free Surface (FS).

Fig. 7b shows the cross section of the sample C. A 2 μm thick crack is visible in the epoxy layer between the 3rd and the 4th ply, in agreement with the computation shown in Fig. 5b. The rupture, mainly in mode I (tensile stress) is interlaminar since it has occurred within the interply. This shows that the tensile strength of the interply is lower than the ply one, especially as the interply is subjected to a slightly lower tensile stress. The delamination is spread over a smaller area than the laser spot due to the lateral attenuation of the stress waves [32]. The damage is not continuous within the interply layer and the plies remain stacked, this could be considered as a first stage of damage. It is possible that the adhesion properties of the interply are heterogeneous due to fibre distribution, thickness variations or residual stresses generated during the cooling after the curing.

These observations confirm that laser-induced stress waves can produce on-axis tension able to delaminate the specimens. This also validates the analysis of the free surface velocity.

Since SEM observation is destructive and limited to a bidimensional view, the microtomograph X-Tek HMXST 225 (Industrial Materials Institute, National Research Council Canada) with a 2 μm precision, is used to examine the recovered samples. Fig. 8 shows the cross sections of the 4 ply samples A, D and E after an impact near the delamination threshold, the anisotropic damage is observed within the delamination plane on pictures on the top of the figure.

Fig. 8a confirms that no damage has been induced within the sample A below the damage threshold. Sample D shows thin

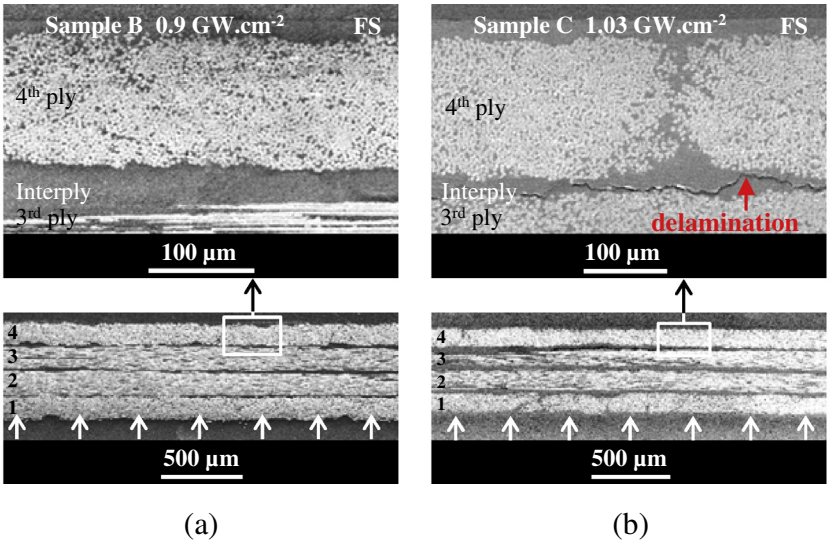

Fig. 7. Microscopic transverse observations of 4 ply laminates. The incident irradiation is: (a) 0.9 GW cm^{-2} sample B without delamination, and (b) 1.03 GW cm^{-2} sample C with shock-induced delamination. The loading zone is indicated by the white arrows.

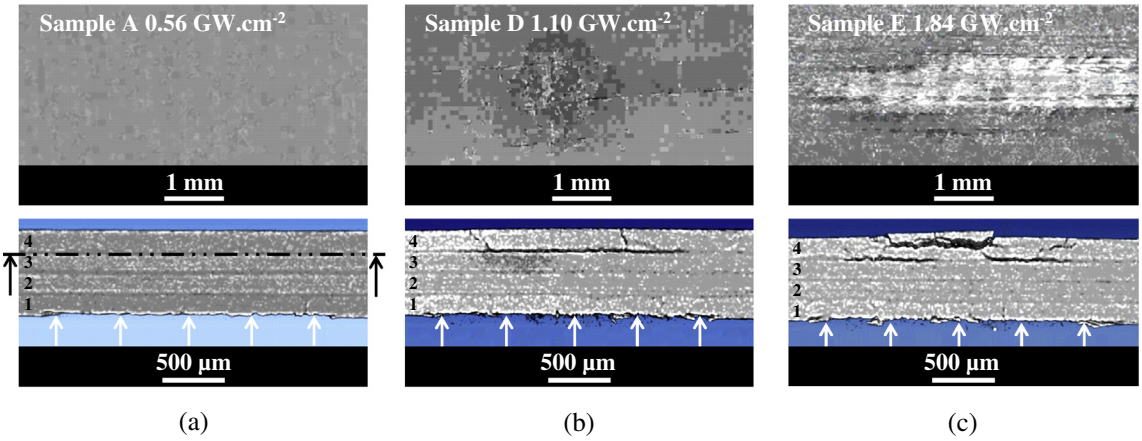

Fig. 8. Microtomographies of 4 ply laminates. The incident irradiation is: (a) 0.56 GW cm^{-2} sample A without delamination, (b) 1.10 GW cm^{-2} sample D, and (c) 1.84 GW cm^{-2} sample E with shock-induced delamination. The loading zone is indicated by the white arrows. The bottom pictures are given in the through-thickness plane, those on top in the delamination plane (the cutting plane is indicated by the black arrows on the bottom left image).

intralaminar delamination normal to the interfaces and interlaminar fractures in the epoxy layer between the 3rdand 4th ply. These cracks are thicker than those on sample C (see Fig. 7b), subjected to a lower stress.

For a higher loading (sample E), the delamination is more important. The 4th ply tends to pull out from the laminate. The intralaminar fractures could have been induced by the flexural stress generated during the removal of the last ply. Fig. 8c (upper image) points out that the delamination is spread over a greater area than the laser spot due to the ply anisotropy.

The 3D observation also shows that the delamination is exclusively located in the ply near the back surface.

5. 8 ply laminates behaviour under laser-induced shock load

The study is extended to 8 ply laminates to validate the process for thicker targets. It is also possible to compare the results with tests performed on similar 8 ply samples with a 450 ns pulse duration [34].

When compared to the previous case, the 8 ply samples have more interfaces, leading to further wave reflections. According to relation (2), the interfaces induce a 24.2% decrease of the stress amplitude during the propagation in the 8 ply composite. This yields to a relatively lower tensile stress near the back surface.

Sample F has been subjected to a 1.31 GW cm^{-2} irradiation, this is not sufficient to induce delamination. A stronger irradiation (1.49 GW cm^{-2}) leads to the delamination of sample G.

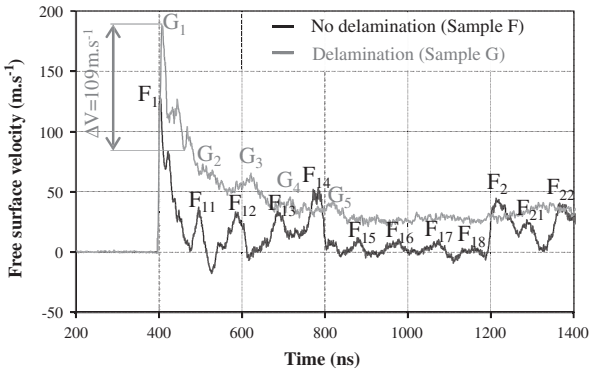

Fig. 9. Experimental free surface velocity of 8 ply laminates from 0 to 1400 ns, without (sample F, 1.31 GW cm^{-2}) and with shock-induced delamination (sample G, 1.49 GW cm^{-2}).

Since the energy of the laser source is limited, the impact size cannot be further increased and its diameter is only 2.1 times larger than the sample thickness. Release waves from the load edge could slightly decrease the on-axis stress.

The free surface velocities recorded during these experiments are given in Fig. 9. The motion of the free surface is again characteristic of the propagation of stress waves.

The first velocity rise F_1 at t = 405 ns is attributed to the arrival of the incident shock at the back surface. The accelerations F_{11} to F_{18} with a 100 ns period correspond to the emergence of the superimposed waves reflected at the numerous interfaces of sample F. The velocity peak F_2 indicates that the sample is intact, since $t_{F2} - t_{F1}$ (about 820 ns) is approximately equal to twice the transit time of the main wave in the laminate:

$$t_{back\ and\ forth} = 2 \times thickness_F / C_{0\ laminate} = 2 \times 1.19 \cdot 10^{-3} / 2890 = 800\,\text{ns}.$$

The velocity profile of sample G has a period of oscillation of about 100 ns, equal to twice the transit time of the wave in the delaminated ply (between the delamination and the free surface). This evidences the shock-induced delamination at the interply 7–8.

The delamination threshold of the 8 ply laminates is evaluated for an incident pressure of [510–570] MPa, i.e., 540 ± 30 MPa (see Section 3.2). The dynamic tensile strength between plies is then calculated at [275–308] MPa, i.e., 292 ± 17 MPa (see Section 3.3). Other experiments performed on the same samples provide a similar strength ([255–296] MPa, i.e., 276 ± 20 MPa, with a 450 ns pressure pulse duration [34]).

Relation (3) provides a dynamic tensile strength of σ_{spall} = 266 MPa with a pullback velocity of ΔV = 191–82 = 109 m s^{-1}. This is in the same range than the computed evaluation (292 ± 17 MPa).

These specimens have been recovered for microscopic observation. Fig. 10a shows SEM transverse observations of sample F after a shock below the delamination threshold. It shows no interface separation.

Fig. 10b shows the shock-induced delamination of sample G. It is still interlaminar near the free surface, this confirms that the interply is weaker than the ply.

These results show that the technique can generate a tensile stress able to delaminate a thicker target. The perspectives of the experiments on 8 ply laminates concern the edge effects: the stress waves propagate normal to the plies when the laser spot is at least three times larger than the target thickness. A higher power pulsed laser is thus required.

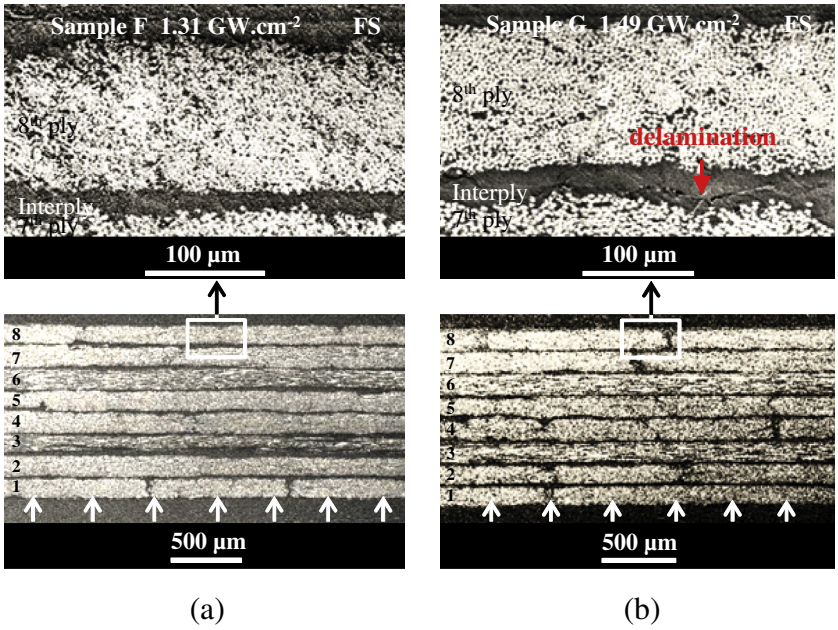

(a) (b)

Fig. 10. Microscopic transverse observations of 8 ply laminates. The incident irradiation is: (a) 1.31 GW cm^{-2} sample F without delamination, and (b) 1.49 GW cm^{-2} sample G with shock-induced delamination. The loading zone is indicated by the white arrows.

Table 3
Delamination threshold of the specimens.

Configuration	Incident laser intensity threshold (GW cm^{-2})	Incident pressure threshold (MPa)	Tensile strength (MPa)	Location of the delamination
4 ply	[0.9–1.03]	[360–430]	[266–318]	Interply 3–4th ply
8 ply	[1.31–1.49]	[510–570]	[275–308]	Interply 7–8th ply

6. Discussion

The main results for the 4 and 8 ply laminates are given in Table 3. The pressure threshold and tensile strength at very high strain rate are evaluated using numerical results (see Sections 3.2 and 3.3).

The incident load required to delaminate the 8 ply samples is higher than for the 4 ply specimens due to the stress wave attenuation. This is mostly attributed to the propagation through the numerous interfaces and to the hydrodynamic damping in a twice as thick sample.

The dynamic tensile limit (mode I) is evaluated at [266–318] and [275–308] MPa, respectively for the 4 and 8 ply laminates. Both samples configurations have similar strength (about 292 MPa). This is in the same range than the strength evaluated by Perton et al. [15] (σ_{spall} = 340 MPa under similar conditions), Yu and Gupta [12] (σ_{spall} = 214 MPa for the CFRP composites Hercules AS4 3502 subjected to a 16–20 ns laser-generated pressure pulse) and Riedel et al. [18] (σ_{spall} = 250 MPa for CFRP composites subjected to a plate impact at a strain rate of 150,000 s^{-1}).

However, the dispersion of the threshold interval is important: the difference reaches 9% of the average for the 4 ply laminates due to the strength variability of the tested specimens.

The adhesion test using laser-induced shock has many advantages compared with the conventional inspection methods. The strength is evaluated in the direction normal to the interfaces, with a quasi-uniaxial deformation (mode I). It remains non-destructive since a calibrated proof-load only fails deficient samples and the wave propagation does not alter the composite properties [16]. It also has the ability to test locally structures of any shape without mechanical contact. In addition, the high power laser systems are now compact and secured for factory implementation.

However, this approach has several limitations. The incident surface of the target has to be protected from the irradiation by black paint, the back surface has to be free. A restriction on the sample thickness also remains due to stress wave attenuation, but some experiments have been successfully performed on 25 mm thick specimens using longer pressure pulses [6].

7. Conclusion

The response of 4 and 8 ply CFRP laminates to a dynamic load normal to the fibres direction has been studied in this paper. The response of the composites is similar in both thickness configurations. It has been demonstrated that laser-induced shock can generate on-axis tension able to delaminate the specimens. The failure or resistance of the laminate during the proof test is determined by an analysis of the free surface velocity. The dynamic strength between plies has been evaluated at 292 MPa on average.

Further works concern the use of high power laser with variable pulse duration, this would give the ability to interrogate the delamination threshold of any interply.

Acknowledgments

This work has been undertaken in the framework of the French CNRS – Canadian CNRC research project SATAC (Shock Adhesion Test for Adhesively bonded Composites). The authors are grateful to the team of Jean-Pierre Monchalin (Industrial Materials Institute, National Research Council Canada) and particularly Christian Néron who performed the microtomographies presented in this study. We acknowledge the IAR (Institute for Aerospace Research, National Research Council Canada) for supplying the CFRP panels. We also thank the DGA (French General Delegation for Armament) for funding the PhD associated to this work (Grant No. 2008333).

References

[1] Adams RD, Cawley P. A review of defect types and nondestructive testing techniques for composites and bonded joints. NDT Int 1988;21(4):208–22.

[2] Vossen JL. Adhesion measurement of thin films, thick films, and bulk coatings. In: Mittal KL, editor. American society for testing and materials, vol. 640. Philadelphia: Special Technical Publications; 1978. p. 122–33.

[3] Gupta V, Argon AS, Cornie JA, Parks DM. Measurement of interface strength by laser-pulse-induced spallation. Mater Sci Eng A 1990;126(1–2):105–17.

[4] Bolis C, Berthe L, Boustie M, Arrigoni M, Barradas S, Jeandin M. Physical approach to adhesion testing using laser-driven shock waves. J Phys D: Appl Phys 2007;40(10):3155–63.

[5] Arrigoni M, Cuq-Lelandais JP, Boustie M, Gay E, Berthe L. An industrial challenge based on the wave propagation: the shock adhesion test. In: Wave propagation. WY (USA): AcademyPublish Ed; 2012.

[6] Bossi RH, Housen K, Walters CT, Sokol D. Laser bond testing. Mater Eval 2009;67(7):819–27.

[7] Arrigoni M, Monchalin JP, Blouin A, Kruger SE, Lord M. Laser doppler interferometer based on a solid Fabry–Perot etalon for measurement of surface velocity in shock experiments. Measur Sci Technol 2009;20(1):015302.

[8] Barker LM, Hollenbach RE. Laser interferometry for measuring high velocities of any reflecting surface. J Appl Phys 1972;43(11):4669–75.

[9] Antoun T, Seaman L, Curan DR, Kanel GI, Razorenov SV, Utkin AV. Spall fracture. New York: Springer; 2003. p. 176–197.

[10] Monchalin JP. Optical detection of ultrasound IEEE ultrason. Ferroelectr Freq Control 1986;33(5):485–99.

[11] Gupta V, Pronin A, Anand K. Mechanisms and quantification of spalling failures in laminated composites under shock loading. J Compos Mater 1996;30(6):722–47.

[12] Yu A, Gupta V. Measurement of in situ fiber/matrix interface strength in graphite/epoxy composites. Compos Sci Technol 1998;58(11):1827–37.

[13] Gilath I, Eliezer S, Shkolnik S. Spall behaviour of carbon epoxy unidirectional composites as compared to aluminum and iron. J Compos Mater 1990;24(11):1138–51.

[14] Gilath I, Eliezer S, Bar-Noy T, Englman R, Jaeger Z. Material response at hypervelocity impact conditions using laser induced shock waves. Int J Impact Eng 1993;14(1):279–89.

[15] Perton M, Blouin A, Monchalin JP. Adhesive bond testing of carbon–epoxy composites by laser shockwave. J Phys D: Appl Phys 2011;44(3):4012.

[16] Gay E. Comportement de composites sous choc induit par laser: développement de l'essai d'adhérence par choc des assemblages de composites collés. Ph.D. dissertation. France: Arts et Métiers ParisTech; 2011. <http://tel.archives-ouvertes.fr/docs/00/66/75/60/PDF/These_GAY2011.pdf>.

[17] Ecault R. Etude expérimentale et numérique du comportement dynamique de composites aéronautiques sous choc laser – optimisation du test d'adhérence par ondes de choc sur des assemblages composites collés. Ph.D. dissertation, ENSMA, Poitiers, France; 2011.

[18] Riedel W, Nahme H, Thoma K. Equation of state properties of modern composite materials: Modelling shock, release and spallation. In: Proceedings of the shock compression of condensed matter. Melville, NY: American Institute of Physics; 2004. p. 701–4.

[19] Hazell PJ, Stennett C, Cooper G. The effect of specimen thickness on the shock propagation along the in-fibre direction of an aerospace-grade CFRP laminate. Composites Part A 2009;40(2):204–9.

[20] Millett JCF, Bourne NK, Meziere YJE, Vignjevic R, Lukyanov A. The effect of orientation on the shock response of a carbon fibre–epoxy composite. Compos Sci Technol 2007;67(15):3253–60.

[21] Zhuk AZ, Kanel GI, Lash AA. Glass–epoxy composite behaviour under shock loading. J Phys IV 1994;4(C8):403–7.

[22] Zaretsky E, DeBotton G, Perl M. The response of a glass fibers reinforced epoxy composite to an impact loading. Int J Solids Struct 2004;41(2):569–84.

[23] Katz S, Zaretsky E, Grossman E, Wagner HD. Dynamic tensile strength of organic fiber-reinforced epoxy micro-composites. Compos Sci Technol 2009;69(7–8):1250–5.

[24] Parga-Landa B, Vlegels S, Hernandez-Olivares F, Clark SD. Analytical simulation of stress wave propagation in composite materials. Compos Struct 1999;45(2):125–9.

[25] Fabbro R, Fournier J, Ballard P, Devaux D, Virmont J. Physical study of laser-produced plasma in confined geometry. J Appl Phys 1990;68(2):775–84.

[26] Berthe L, Fabbro R, Peyre P, Tollier L, Bartnicki E. Shock waves from a waterconfined laser-generated plasma. J Appl Phys 1997;82(6):2826–32.

[27] Fox JA. Effect of water and paint coatings on laser-irradiated targets. Appl Phys Lett 1974;24(10):461–4.

[28] Sollier A. Étude des plasmas générés par interaction laser-matière en régime confiné. Application au traitement des matériaux par choc laser. Ph.D. dissertation. France: Université de Versailles Saint-Quentin-en-Yvelines; 2002. <http://tel.archives-ouvertes.fr/docs/00/08/92/43/PDF/manuscrit.pdf>.

[29] Salzmann D, Gilath I, Arad B. Experimental measurements of the conditions for the planarity of laser-driven shock waves. Appl Phys Lett 1988;52(14):1128–9.

[30] Datta SK. Wave propagation in composite plates and shells. In: Chou TW, editor. Composite materials, vol. 1. Oxford: Elsevier; 2000 [chapter VIII], p. 511–58.

[31] De Résséguier T, Berterretche P, Hallouin M. Influence of quartz anisotropy on shock propagation and spall damage. Int J Impact Eng 2005;31(5):545–57.

[32] Boustie M, Cuq-Lelandais JP, Bolis C, Berthe L, Barradas S, Arrigoni M, et al. Study of damage phenomena induced by edge effects into materials under laser driven shocks. J Phys D: Appl Phys 2007;40(22):7103–8.

[33] Gay D. Matériaux Composites. 5ème édition, Ed. Hermès; 2005.

[34] Gay E, Berthe L, Buzaud E, Boustie M, Arrigoni M. Adhesion test for composite bonded assembly using ramp loads induced by high pulsed power generator. J Appl Phys 2013;114:013502.